A EUROPEAN JOURNAL

CHEMPHYSCHEM

OF CHEMICAL PHYSICS AND PHYSICAL CHEMISTRY

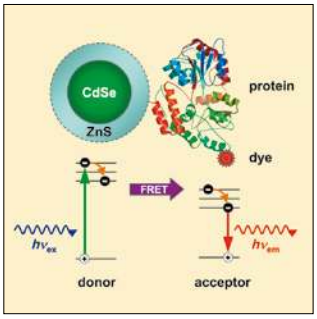

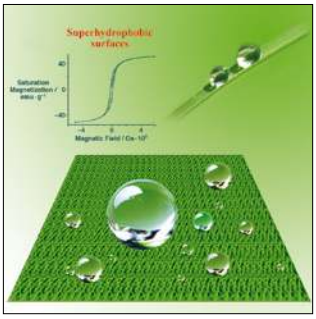

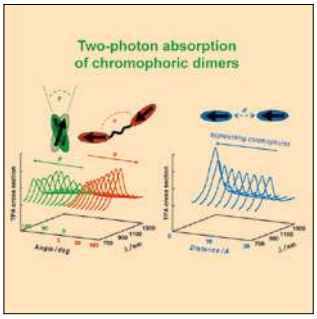

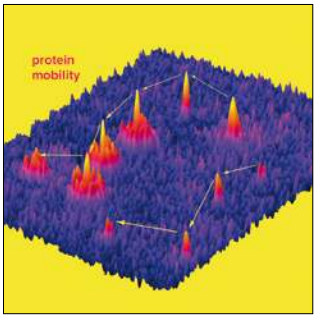

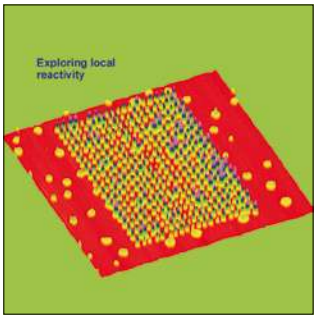

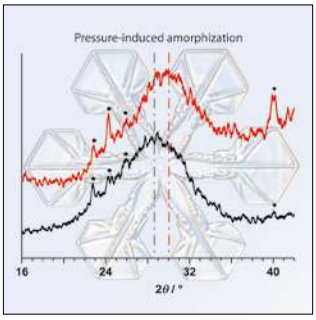

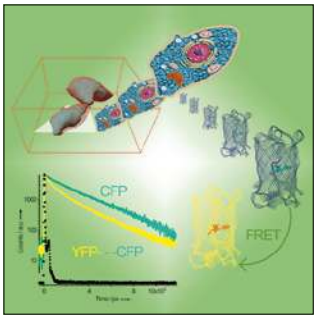

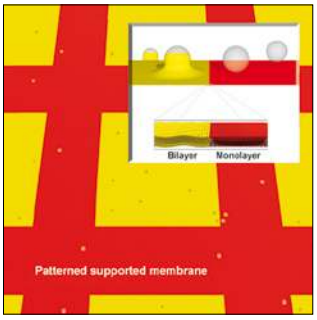

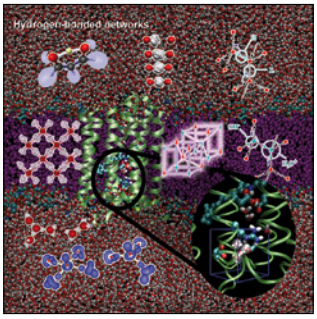

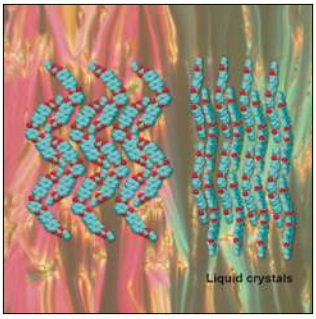

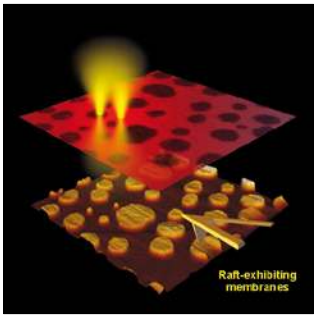

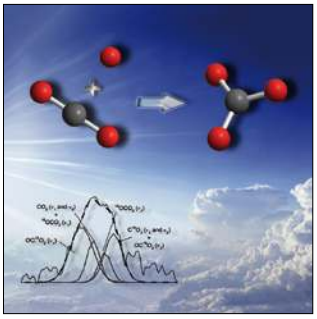

Reprint

WILEY-VCH

A EUROPEAN JOURNAL

CHEMPHYSCHEM

OF CHEMICAL PHYSICS AND PHYSICAL CHEMISTRY

Table of Contents

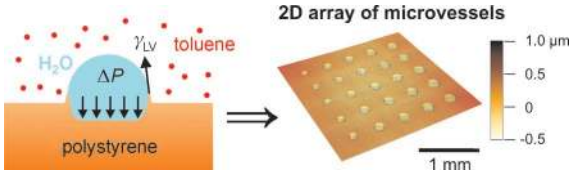

A characteristic microstructure remains on a polymer surface after evaporation of a sessile water droplet in a solvent-rich environment. Regular arrays of size-controlled microvessels are fabricated in this way (see picture). The resulting height profiles are modeled by using a recent elastic theory that is based on the interplay between the interfacial tension γ_{LV} and the Laplace pressure ΔP of the liquid.

WILEY-VCH

CHEMPHYSCHEM

DOI: 10.1002/cphc.200800098

Microstructuring of Polystyrene Surfaces with Nonsolvent Sessile Droplets

Ramon Pericet-Camara, Elmar Bonaccurso,* and Karlheinz Graf*[a]

Herein, we study the microstructuring of toluene-vapor-softened polystyrene surfaces with nonsolvent sessile droplets. Arrays of microvessels are obtained by depositing non-evaporating droplets of ethylene glycol/water on the original polystyrene surfaces and subsequently exposing them to saturated toluene vapor. The droplets act as a mask on the polymer, thereby impeding the toluene vapor to diffuse and soften the polystyrene surface below them. Alternatively, the formation of microcraters at random positions—with an average depth-to-width aspect ratio of 0.5 and a diameter as small as 1.5 μm—is achieved by condensing water droplets on a softened polystyrene surface. The cross-sections of the microvessels and the contact angle of the sessile water droplets suggest that the structures are formed by the combined action of the Laplace pressure at the bottom of the droplet and the surface tension acting at the three-phase contact line of the droplets. As a support, the rim height and the depth of the microvessels are fitted with an elastic theory to provide Young's modulus of the softened polystyrene surface.

1. Introduction

The ability to fabricate small cavities on solid surfaces is important for the development of chemical, electrical or optical microdevices. These cavities are used as templates for the fabrication of micro- and nanopillars[1] or -lenses,[2,3] as microreactors,[4,5] or to facilitate electrical contacts.[6] Micro- and nanoreactors allow synthesizing smaller quantities of reagents, for example, for the build-up of chemical libraries.[7] Additionally, shorter diffusion times and a more efficient heat dissipation are achieved in microreactors. For the use of cavities as templates for optical microlenses, their aspect ratio (depth-to-diameter) must be accurately defined by the fabrication process.

An increasingly used technique is ink-jet etching,[6,8,9] where solvent droplets are deposited on polymer surfaces through an ink-jet nozzle. After evaporation of the droplet, a crater-shaped surface topology is left. This surface structure is formed owing to a flow of the dissolved polymer to the rim of the pinned evaporating droplet.[6,10,11] The shape of the microvessels is additionally governed by the surface tension of the droplet acting at the three-phase contact line (TPCL), by the Laplace pressure at the bottom of the droplet, by swelling, by dissolution of the polymer into the solvent drop, and by instabilities.[3,12–14] With ink-jet etching, microvessels with diameters down to 20 μm and aspect ratios of up to 0.07 have been obtained.[8,15] The capability of this technique to produce smaller structures with higher aspect ratios is limited to a great extent by the diameter of the deposited droplets.

To better understand the physics behind the structuring of soft surfaces, we simplify the structuring procedure by using droplets of nonsolvents. In this way, the evaporation-induced flow of polymer to the rim of the droplet is suppressed, while crater-shaped structures still occur. Two complementary experiments are performed, which either focus on the role of solvent uptake, that is, swelling, or on the role of the Laplace pressure and surface tension of the droplet for structuring. In the first experiment, slow evaporating microdrops of a mixture of ethylene glycol and water (EG/H_2O) are deposited on a polystyrene (PS) surface by the ink-jet technique. After that, they are exposed to saturated toluene vapor to swell and soften the polymer surface. In the second experiment, the PS substrate is pre-softened by exposing it to solvent vapor before droplets of pure water are condensed onto it.[15]

We show that part of the structuring results from the permanent uptake of solvent, which can be considered as the opposite to the structuring by compaction.[16] Additionally, we demonstrate that the combination of the surface tension and the Laplace pressure of the droplet leads to crater-shaped structures with aspect ratios of 0.5, even for the system toluene/PS. The resulting height profile is discussed on the base of an elastic theory.

Experimental Section

Polymer: Extruded polystyrene (PS) plates ($M_w = 310$ kDa, $M_w/M_n =$ PDI (polydispersity index) $= 2.07$;[1] GoodFellow GmbH, Bad Nauheim, Germany) were cut into 2.5×7.5 cm^2 slices and ultrasonicated in methanol (pro analysi, Riedel de Haën, Seelze, Germany) for 5 min to obtain a defined, clean polymer surface. Two different structuring procedures were applied. In the first experiment, the droplets were deposited on top of the original PS surface and after that the PS substrates were exposed to toluene vapor. In the

[1] *Measured by Sandra Seywald and Beate Müller, Max Planck Institute for Polymer Research, Mainz*

[a] *Dr. R. Pericet-Camara, Dr. E. Bonaccurso, Dr. K. Graf*
Max Planck Institute for Polymer Research
Ackermannweg 10, 55128 Mainz (Germany)
Fax: (+49) 6131-379-310
E-mail: grafk@mpip-mainz.mpg.de
bonaccur@mpip-mainz.mpg.de

second experiment, the polymer substrates were exposed to toluene vapor and after that water droplets were condensed on top of the softened polymer surface.

Droplet Deposition (Experiment I): Microdrops of a 1:1 mixture of ethylene glycol (≥99.5%, Riedel de Haën, Seelze, Germany) and ultrapure water ($\rho \approx 18.2$ MΩ·cm; Arium 611, Sartorius AG, Göttingen, Germany) were deposited by means of the ink-jet technique on the PS substrates with a Nano-Plotter NP 2.0 (GeSiM GmbH, Grosserkmannsdorf, Germany), which consists of a mobile pipette dispenser and a working plate. The dispenser is a software-controlled, piezoelectric driven microdosage head with a computer-controlled positioning system. The droplets were deposited on the polymer substrate in a 5×5 square array. Mixing with pure water was necessary because the viscosity of pure ethylene glycol was too high for a proper dispensing at room temperature.[17]

With this technique, square arrays of EG/H_2O droplets were deposited at a distance of 500 μm. The PS surface bearing the droplet array was then exposed to toluene vapor in a closed cell for a fixed time. After that, the cell was opened and the surface was left overnight for complete evaporation of the toluene and the EG/H_2O droplets. Finally, the surfaces were carefully rinsed with pure water and dried gently in a stream of nitrogen to eliminate the visible rests of ethylene glycol (this procedure does not affect the surface topology).

Droplet Condensation (Experiment II): For softening of the polymer surface, a saturated toluene atmosphere was prepared in a closed glass cell. A piece of filter paper was placed around the polystyrene plate with a tweezer and soaked with toluene (99.7%, Riedel de Haën, Seelze, Germany) using a syringe. Saturation with toluene vapor was maintained by keeping the filter paper wet during the exposure. For the condensation of water droplets on the PS substrate, it was placed on a Peltier element (Elektronik Labor, Neuenkirchen, Germany) inside the glass cell, separated by a thin microscope cover glass to avoid sticking of the softened PS plate. The surface of the polystyrene with the condensed droplets was observed from above during the treatment with toluene vapor with reflected light microscopy (Zeiss Axiotech, Carl Zeiss AG, Germany).

Surface-Topography Measurements: For experiment I, the surface topology of the PS substrates was visualized with a μSurf white-light confocal profilometer (Nanofocus AG, Oberhausen, Germany) because the size of the surface structures was beyond the range of the AFM. For a 20x objective, the nominal resolution of the profilometer was determined as 1.57 μm horizontal to the substrate surface (*X*-*Y*) and has—according to the manufacturer—a resolution of 5 nm perpendicular to the substrate surface (*Z*-direction).

For experiment II, the surface topology of the PS surface was imaged with a Nanowizard (JPK Instruments AG, Germany) atomic force microscope (AFM) in intermittent-contact mode. Cantilevers (OMCL-AC160TN-W2, Olympus, Japan) with a nominal spring constant of $k = 42\ \mathrm{N\,m^{-1}}$ and a resonance frequency of $f = 300$ kHz were used. After a plane-fit, the images were analyzed with the assistance of a software (Igor Pro, Wavemetrics, USA).

2. Results and Discussion

2.1. Microstructures Obtained by the Deposition of Ethylene Glycol/Water Droplets

In the first set of experiments, we investigate the exposure of polystyrene (PS) substrates to toluene vapor in the presence of non-evaporating liquid sessile droplets. Firstly, a 5×5 array of ethylene glycol/water (EG/H_2O) droplets with diameters between 100 and 200 μm is prepared. The droplets are deposited with the ink-jet technique on the PS surface, thereby controlling their size and position. The diameter is changed by depositing different numbers of droplets on the same spot. Secondly, the PS surface with the array of droplets is exposed for different times to toluene vapor. The droplets prevent the penetration of toluene into the polymer at the contact area between droplet and polymer surface (see Figure 1a). Thus, toluene can only diffuse into the noncovered polymer surface, which leads to uptake of vapor and thus to a vertical expansion of the polymer (see Figure 1b).

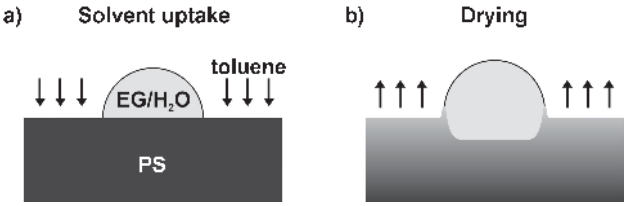

Figure 1. Schematics of a) the diffusion of toluene (arrows) into a polystyrene (PS) substrate, covered with a sessile drop of a 1:1 mixture of ethylene glycol and water (EG/H_2O) and b) drying of the expanded polymer surface.

Figure 2a shows the surface topology of the array imaged with confocal white-light profilometry after vapor uptake, consecutive drying, and final removal of the droplets. The number of EG/H_2O droplets deposited on one spot increases from one to five from left to right along one row.

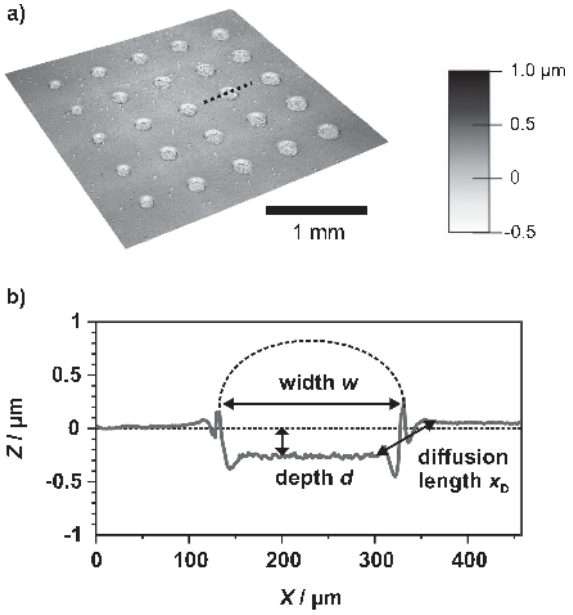

Figure 2. a) Array of structures formed on a polystyrene substrate masked by ethylene glycol/water droplets after exposure to toluene vapor for 3 min. b) Profile of the microcavity along the dotted line in (a). The droplet is indicated as a dashed line (not to scale). The diffusion length is defined as the minimum distance over which toluene diffuses under a particular droplet (see text).

After exposure to toluene, circular surface structures are visible, which correspond to the contact area with the droplet. Their diameter increases with increasing number of deposited droplets on one spot. A typical height profile of a single microstructure is shown in Figure 2b. The bottom of the craterlike structure is deeper than the surrounding PS surface and a rim of PS is formed at the edge of the restructured surface with dimples around it. The root-mean-square (RMS) roughness inside the structure is 9 nm compared to 7 nm in the toluene-exposed PS surface. Comparing the surface roughness for all structures shows a nearly constant surface roughness of 8.4 ± 0.6 nm inside the microcraters, whereas it decreases from 17.0 to 5.5 nm with increasing exposure time in the area around the structures.

The profiles show a nonlinear increase of the depth of the microcraters with increasing exposure time to toluene vapor (Figure 3a).

This result suggests that the evolution of a height difference between the uncovered PS substrate and the one below the droplet is generated by a permanent uptake of toluene. The longer the substrate is exposed to toluene vapor, the more toluene diffuses into the PS substrate and the more it stays in the uncovered PS substrate. Several hints support this interpretation.

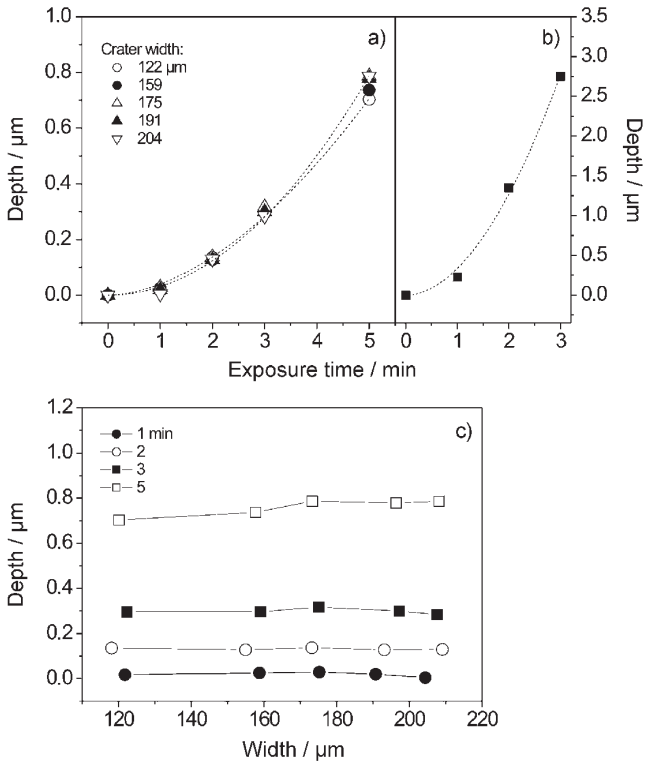

Figure 3. a) Depth d of the microcavities formed by the EG/H_2O droplets during exposure to toluene vapor as a function of the exposition time t. The widths of the microcavities are taken from (c). The dashed lines are fits with power series. b) Depth of microvessels fabricated in PS after exposure to 25 vol.% toluene in ethanol and drying.[18] c) Depth d of the microcavities as a function of their width w. The legend shows the corresponding exposure times to toluene vapor.

Firstly, a permanent uptake of toluene in the order of $\approx 3\%$ was measured for a microsized PS particle and for PS films on solid supports[19,20] (the radius of the particle increased permanently). Secondly, the same behavior was found in an earlier work on the fabrication of an array of microvessels in a PS surface with a different technique, but also based on the uptake of toluene (Figure 3b).[18] The stronger increase in the depth with the exposure time to toluene is because toluene is offered as a liquid in 25% mixture with ethanol. Thus, the polymer is in permanent contact with the solvent and decoupled from environmental influence. A third hint is the independence of the crater depth on its width (see Figure 3c). This suggests that most of the polymer under the droplet is unaffected by the entering solvent molecules and only the noncovered PS comes into contact with the solvent. Accordingly, the RMS surface roughness of the polymer under the droplet remains constant, whereas that of the uncovered PS decreases with the exposure time to the solvent. The interfacial tensions of PS/air (≈ 43 mN m^{-1} at 20 degrees) and PS/water are in the same order of magnitude[21] and thus cannot contribute to differences of the RMS roughness. Therefore, the flattening in the uncovered PS surface indicates that only this part came into contact with the toluene vapor.

The changing RMS roughness along the PS surface quantitatively supports the idea that the structuring occurs because of a permanent uptake of solvent, initiated by diffusion. To this end, we measure the lateral diffusion length x_D of toluene into the PS surface. From x_D the step-height of the resulting microcraters, that is, their depths, can be estimated, because the relative amount of toluene permanently trapped in PS was determined from an independent experiment.[19,20] The diffusion length is derived from the lateral distance between the contact point of the droplet on the surface and the bottom of the microcrater under the droplet with a roughness comparable to that of the uncovered PS (Figure 2b). The error from neglecting the rim height is 7%. The parameter x_D represents the minimum length over which the toluene diffuses into the PS. The surface roughness only decreases if the polymer is above the glass transition point. This occurs if sufficient solvent diffuses into the polymer, thus leading to plasticization.[22] In our system, this is the case for concentrations above $\approx 30\%$ of toluene in PS.[23] Figure 4a shows a plot of the diffusion length versus the exposure time to toluene vapor.

The diffusion length increases with increasing exposure time to toluene vapor. This is reasonable, since the solvent is accumulated in the PS with increasing exposure time. Thus, after drying, an increased residual of solvent and increased depth of the microcraters can be expected. From the diffusion length x_D, the diffusion coefficient D can roughly be estimated according to $D = x_D^2/6t$ (Figure 4b), where t is the exposure time to toluene vapor.

The diffusion coefficient increases with t. The more solvent is accumulated in the polymer, the higher must be the diffusion coefficient, because the polymer–toluene mixture becomes increasingly liquidlike. The size of the diffusion coefficient is between that of a polymer ($M_w = 340$ kDa) in a toluene-rich PS matrix with $M_w = 220$ kDa ($D = 2 \times 10^{-13}$ m^2 s^{-1})[24] and

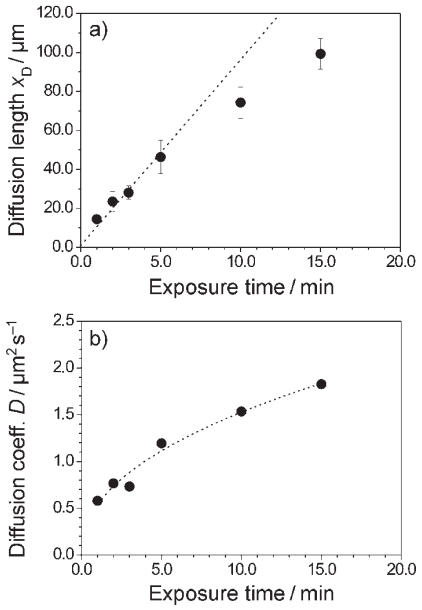

Figure 4. a) Diffusion length of the microcavities formed by EG/H_2O droplets during toluene-vapor exposure as a function of the exposition time *t*. b) Averaged diffusion coefficients *D* derived from (a) as described in the text. The line is a fit with a power law.

that for toluene in toluene ($D \approx 3 \times 10^{-9}$ m^{2}s^{-1}).[25] The value is in good agreement with that of about 10^{-12} m^{2}s^{-1} obtained from recent fits[26] of data from a swelling PS particle in toluene vapor.[19] To derive the vertical depth of the microcraters, we assume that the diffusion is isotropic. Thus, the toluene might diffuse at least about 28 µm into the PS surface after 3 min. We expect a permanent volume change of approximately 103%.[19,20] Therefore, a volume of 28^3 µm^3 will have a volume of 1.03×28^3 µm^3 after swelling and drying. This leads to an increase in height of $[(\sqrt[3]{1.03} \times 28) - 28] \approx 280$ nm after drying, which is in good agreement with the actually measured depth of the corresponding microcrater of approximately 320 nm (Figure 3a). After 5 min of exposure to toluene vapor, the depth should be $[(\sqrt[3]{1.03} \times 46) - 46] \approx 460$ nm after drying. Even if this value is about 300 nm below the corresponding depth in Figure 3a, it is a reasonable value. In the way the diffusion length is analyzed, only toluene concentrations, which actually lead to a softening of the PS, are considered (see discussion above). Moreover, the uptake of toluene leads to an expansion of the polymer. Thus, the actual diffusion length during the exposure to solvent will be higher. Therefore, the exact dependencies shown in Figure 4 should not be taken for granted. A more refined analysis, where expansion of the polymer is included in the analysis, is under preparation.[26]

In summary, the formation of microcraters can be consistently explained by a permanent uptake of toluene (of the order of some vol%) by the PS surface not masked with the EG/H_2O droplets. The area outside the drops grows in height, whereas the area underneath the drops remains unchanged. In this case, the structuring process is opposite to the compaction mechanism proposed in the literature.[16]

2.2. The Rim Height

Small spikes with heights of the order of several 100 nm are visible at the TPCL (see Figure 2b). While the step forming the microcraters can be explained consistently with a permanent trapping of solvent in the polymer, the spikes indicate the presence of a force acting on the polymer surface. This force is exerted at the rim of the droplet, and thus, it most probably originates from the surface tension of the droplet. This interpretation is only valid if the force is acting on the polymer surface during the whole time of the experiment at the same position, that is, the radius of the droplet must be constant. Furthermore, the vertical component of the force acting on the polymer surface is nonzero only if the contact angle of the droplet is also larger than zero. Both requirements are fulfilled (see Figure 5a).

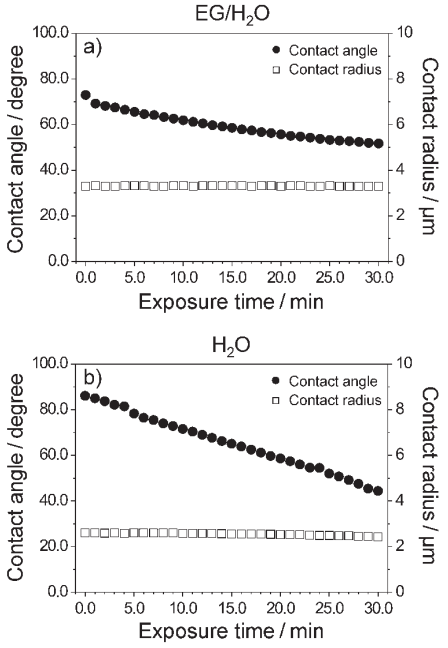

Figure 5. Contact angle (●) and contact radius (□) of a sessile droplet as a function of the exposure time to a saturated toluene atmosphere for a) a droplet from a mixture of ethylene glycol and water (50% w/w) and b) a pure water droplet.

Indeed, the contact radius of the droplet is nearly constant (≈3.3 mm), which shows that the droplet is pinned at the TPCL. The contact angle decreases only slightly from about 72 degrees to about 60 degrees after 15 min. This decrease can be attributed to the slow evaporation of water from the droplet. Thus, the rim of the droplet actually exerts a force on the softened PS, owing to the surface tension γ_{LV} at the air–liquid interface of ≈ 50 mN m^{-1} for EG/H_2O,[27] thus pulling the polymer upwards.

As a further support for this idea, Young's modulus of the PS substrate is estimated from the rim height, *h*, with the elastic theory proposed by White.[28] This theory describes the deformation of an elastic surface by a competition of the surface tension γ_{LV} and the Laplace pressure of the droplet (Figure 6).

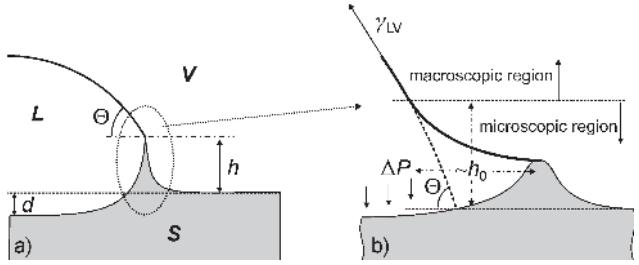

Figure 6. a) Scheme of the deformation of an elastic surface by a sessile droplet (*L*, *S*, and *V* stand for liquid, solid, and vapor, respectively). The dotted line displays the solid surface without deformation. The parameter θ is the equilibrium contact angle of the droplet, *h* is the maximum height of the ridge, and *d* is the maximum depth of the depression under the drop. b) Magnified scheme of the contact point at the TPCL. The surface tension pulls at the ridge and the disjoining pressure Π acts locally at the interface over a distance h_0, which can be defined as the range over which the meniscus is bent owing to the van der Waals interaction with the substrate. The value ΔP is the Laplace pressure leading to a depression.

The surface tension leads to a deformation towards the droplet, while the Laplace pressure ΔP leads to a depression in the center. The rim height *h* is given by Equation (1):

$$h = \frac{2\gamma_{LV}(1-\nu^2)}{\pi E}\left\{\sin\theta\left[4(\ln 2 - 1) - \ln\left(\frac{4h_0}{w}\right)\right] + \int_0^{w/2} \mathrm{d}r \frac{\Pi}{\gamma_{LV}} \ln\left(\frac{w/2 - r}{h_0}\right) + O\left[\frac{h_0}{R}\ln\left(\frac{h_0}{R}\right)\right]\right\} \quad (1)$$

where ν and *E* are the Poisson ratio and Young's modulus of the polymer substrate, respectively. Other parameters are the contact angle, θ, the vertical range of the disjoining pressure, h_0, the radius of curvature of the droplet, *R*, the width of the microcrater, *w*, and the disjoining pressure, Π. The second part of the equation describing the influence of the disjoining pressure by integration over the droplet radius *r* can be neglected, as estimations show for $\Pi = 1000$ Pa and $h_0 = 0.1$ μm.[29] With a surface tension of $\gamma_{LV} = 50$ mN m^{-1}, droplet widths of 120 μm, an average contact angle of 65 degree, a Poisson ratio of 0.354 for nonsoftened PS,[30] and a rim height of 250 nm (Figure 2b), Young's modulus is in the range of about 440–800 kPa. This is in good agreement with data from literature for gel-like polymers.[28,31] The error that derives from assuming a constant contact angle is in the order of only 5%.

On the other hand, the removal of the EG/H_2O droplets from the nonsoftened PS leaves a flat polymer surface behind. Without the possibility of freezing the deformed polymer surface through fast solvent evaporation, any elastic deformation of the surface is reversible. Additionally, according to Equation (1), in a nonsoftened PS surface, a maximum rim height of only about 36–67 nm can be expected owing to the high Young modulus (of ≈3 GPa).[32,33] This is at the limit of the resolution of the confocal microscope.

Principally, the dependence of the rim height on the width of the concave structure can also be described by the theory of Shanahan and de Gennes.[34] For the net deformation $\delta u_z(x)$ of a soft substrate, that is, the deformation at the rim x_0 of the droplet minus the deformation far away, at *x*, the authors provide Equation (1a):

$$\delta u_z(x) = u_z(x_0) - u_z(x) = \frac{2(1-\nu^2)\gamma_{LV}}{\pi E}\ln\frac{x}{x_0} \approx h \quad (1a)$$

Here, x_0 is interpreted as the lateral distance over which the force at the rim of the droplet is acting. If we interpret $\delta u_z(x)$ as our rim height *h* and *x* as the width of the concave structure, which actually is far away from the rim of the droplet, we obtain after rearrangement of (1a) Equation (1b):

$$h = \frac{2\gamma_{LV}(1-\nu^2)}{\pi E}[\ln w - \ln(2x_0)] \quad (1b)$$

For $\theta = 90°$—and neglecting the second term in Equation (1)—a comparison between Equations (1b) and (1) reveals that $h_0 = 2x_0/13.65$. Even if this relation cannot be taken as the exact result owing to the rough approximations it nevertheless shows that 1) both quantities are in the same order of magnitude, which is true, and 2) the principal relation between the rim height and the width of the concave structures can correctly be described with the older theory. However, in White's theory only measurable quantities are provided, whereas Shanahan's theory contains the free adjustable parameter x_0.

The dimples around the spikes might occur as a result of the stress gradient at the edge of the droplet during drying and is related to the elasticity of the material.[35,36] Similar structural features were found during the structuring of polymer surfaces with solvents during drying in presence of an abrupt change in the mechanical surface properties, as was realized for locally cross-linked or gold covered polymer surfaces.[18]

In summary, the spikes occurring in the height profile across the structured PS surface can be understood on the base of an elastic theory. This shows that they occur as a result of the force exerted by the droplets on the polymer substrate. Young's modulus of the softened PS surface is calculated from the elastic theory and is found to lie in a reasonable range. However, the Laplace pressure does not cause the expected depression in the PS surface. This can have two reasons: Firstly, the radius of the droplet is so big that it leads to a pressure in the order of only 7 mbar; secondly, as shown above, the PS under the droplet was not softened. Thus, it is too stiff to be affected by the Laplace pressure.

Structuring of the PS surfaces with toluene vapor in the presence of relatively large sessile droplets shows that the aspect ratio of the resulting microcraters (smaller than or equal to about 7×10^{-3}) is very low (see Figure 3a,b). This is owing to the slow diffusion of toluene into the PS under the drop, which thus is not allowed to be softened. If the drop size on the other hand would be smaller than about 30 μm, which is twice the diffusion length found above (Figure 4a), the polymer under the drop should become softer and allow the formation of depressions by the action of the Laplace pressure. Being able to reduce the width to 1 μm thus would provide an

aspect ratio of approximately 0.7. Unfortunately, the ink-jet technique used for the big droplets cannot be used to generate such small drops. We achieve this by condensation of water drops on softened PS instead.

Microvessels Obtained by Water-Droplet Condensation

The influence of the droplet size on the aspect ratio of the microvessels formed on the softened PS surface is investigated by random condensation of water microdrops on the surface. In this way, many droplets of different sizes are formed simultaneously, which offers the possibility of a statistical analysis under constant boundary conditions. In contrast to the ink-jet technique, the dependence of the droplet diameter from the size of the nozzle is overcome.[8] Water is a non-solvent for PS and it possesses a high surface tension and contact angle versus PS. Therefore, the deformation of the surface due to the surface forces described above will be at maximum, since the contact angle of water on PS is between 80 and 90° (see Figure 5b).

During the condensation of a water droplet on the softened PS surface, different process parameters can be important: 1) the degree of softening of the polymer in toluene vapor before the droplet condenses, 2) the contact time of the droplet with the softened PS surface, and 3) the evaporation time of the droplet compared to the drying time of the toluene-rich PS. All three are varied in the following experiment to control the softening of the polymer and the formation, the growth and the evaporation of the microdrops. The PS substrate is placed on a Peltier element, tempered at 0 °C, in a closed glass cell in saturated toluene vapor. Even after 5 min, no water droplets condense on the PS surface, regardless of whether the Peltier element is cooled down from room temperature (22 °C) before or after the substrate is placed inside the cell. After different waiting times ($\approx$1 min, 5 min), the cell is opened partially and thus exposed to the ambient atmosphere. After a few seconds, small droplets cover the entire PS surface, and after that, the cell is closed again. The size of the droplets is stable over the whole experiment. After different times ($<$1 min, 2–3 min), the cell is opened completely and the temperature is set to 30 °C. The droplets evaporate and circular microvessels with a diameter comparable to that of the droplets are left.

This set of experiments shows that condensation can only occur after a decrease of the toluene vapor concentration and/or the increase of humidity in the cell. Thus, the condensation must be that of water from the ambient air. When the temperature of the surface is 0 °C, the formation of droplets on the surface always occurs briefly after opening the cell, independently from the exposure time to toluene vapor. A condensation of toluene drops is never observed. This is in contrast to the findings for structuring of poly (methyl methacrylate) (PMMA), where the solvent was claimed to condense on the polymer.[16] As we will show, the condensation of water on the softened PS can lead to aspect ratios of about 0.5, without the need for compaction or a flow of polymer to the rim, as induced by a coffee-stain-like effect.

The size of the water droplets influences the geometry of the microvessels after evaporation. This is visualized with an atomic force microscope (AFM) working in the intermittent-contact mode. A typical image of the PS surface after 5 min of exposure to toluene vapor and 2–3 min of contact with the condensed drops is shown in Figure 7a.

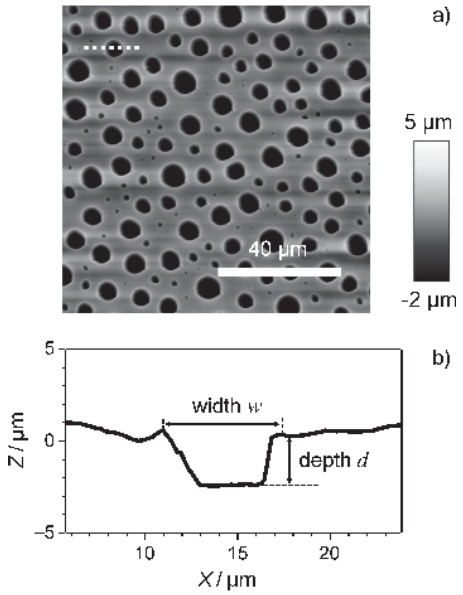

Figure 7. a) Atomic force microscopy image (taken in intermittent-contact mode) of a dried polystyrene surface after a 5 min exposure to toluene vapor and consecutive condensation of water microdroplets. b) Typical height profile of a microvessel along the dashed white line in (a).

The image shows dark, irregularly distributed, nearly circular areas, which correspond to the contact area of the condensed water droplets. Their diameters range from 1 to about 10 µm. A typical height profile, taken along the white dashed line in Figure 7a, is shown in Figure 7b. The U-shaped microvessel shows a low rim, the whole structure resembling a crater as for the case of larger EG/H_2O droplets. The rim height (of the order of some 100 nm) is much lower than the depth of the crater (which is several micrometers). A similar profile, although for pure elastic surfaces, was previously proposed by Rusanov[37] and White.[28] Two main forces deform elastic surfaces. The surface tension γ_{LV} at the liquid–vapor interface of the droplet pulls upwards at the TPCL, thus forming a rim, as described for the droplets of EG/H_2O. Additionally, the Laplace pressure ΔP pushes downwards at the bottom of the droplet, thereby deepening the region with respect to the surrounding area. Both features are found in the experimental profile in Figure 7b. In contrast to the droplets of EG/H_2O, the surface roughness inside and outside the microvessel is the same, because the toluene vapor is applied prior to droplet deposition. Therefore, the action of the Laplace pressure produced a measurable effect in this case. For a quantitative comparison, we calculate the rim height [see Eq. (1)] and the depth of the microvessel, as suggested by White (see Figure 6). The depth, *d*, is given by Equation (2):

$$d = -\frac{2\gamma_{LV}(1-\nu^2)}{E}\left[\sin\theta + O\left(\frac{h_0}{R}\right)\right] \quad (2)$$

The parameters are the same as those in Equation (1). The width of the crater is defined as the horizontal distance between the summits of the rim and the depth as the vertical distance between the surface outside the structure and the bottom of the cavity (see Figures 7b and 2b). With an average contact angle of water on PS of about 80° (Figure 5b), a surface tension of approximately 73 mN m^{-1} for water at 20 °C,[38] a Poisson ratio of 0.354 for nonsoftened PS,[30] a depth of 2.5 μm, and $h_0 \ll R$, Young's modulus results to be 50 kPa, which is about one order of magnitude lower than that for the droplet deposition of EG/H_2O, because the PS is exposed to toluene *prior* to the deposition of the droplet, and is thus softer. The Laplace pressure deforms the PS surface under the drop, which in fact leads to higher depths compared to those obtained through structuring by swelling. Consequently, the aspect ratio here is about 0.34 (see Figure 7b), which is much larger than that reported above. If only the reduced width would contribute, the aspect ratio would be (0.75 μm/6.3 μm) ≈0.12 (see Figure 3a for the 5 min case). This shows that the aspect ratio of the present microcraters results from a combination of the reduced width and the action of the Laplace pressure.

To cross-check the validity of the elastic theory model by White, we calculate Young's modulus from the rim height as well [Eq. (1)]. As for the droplets of EG/H_2O, we neglect the integral containing the disjoining pressure. With $h_0 = 0.1$ μm, a width of 6.3 μm, an averaged rim height of $h = 250$ nm, and all the other values takes as for Equation (2), Young's modulus is ≈246 kPa. This value, however, is about five times larger than that calculated from the depth. This mismatch can be understood by considering the evaporation of the water droplet. When the cell is opened, the droplet evaporates quickly. Simultaneously, toluene slowly diffuses out of the PS. The rim height must decrease, because the action of the surface tension decreases with decreasing contact angle of the drop (Figure 5b). Therefore, the actual height in the presence of the water droplet must be higher, which leads to a lower Young modulus. Summarizing, the structuring of softened PS surfaces by condensing water droplets can be partially explained on the base of the elastic theory. The depth of the structure is mainly determined by the Laplace pressure, whereas the rim height is governed by the action of the droplet pulling at the TPCL. Both effects are related to the surface tension of the droplet. The higher it is, the higher will be the rim and the deeper the depression.

A further hint for an elastic contribution to the surface structuring of the softened PS by the water droplet can be derived from the dependence of the rim height on the width of the surface structures [see Equation (1)]. Figure 8 shows this dependence for two different exposure times to toluene, that is, two differently soft PS surfaces.

The rim height increases with the width of the microvessels, and thus, with the diameter of the sessile water droplet. Both curves in the plot can be fitted to Equation (1) after rearrangement to $h \approx A\{\sin 80 \cdot [4(\ln 2 - 1) + \ln w] + B\}$, with the fit parameters $A = 2\gamma_{LV}(1-\nu^2)/\pi E$ and B. Here, B contains all terms characterizing the influence from the disjoining pressure, that is, h_0 and the integral. The contribution from the integral is considered to be constant, owing to the small value of h_0. The contact angle is set to 80° and the Poisson ratio to 0.354. From the fits, we obtain $A = 0.261$ μm, $B = 0.488$ and $A = 0.336$ μm, $B = 0.828$ for the short and long exposure times to toluene, respectively. From the values of A, we calculate Young's modulus for the soft PS surfaces, thereby obtaining 156 and 121 kPa, respectively. These values of the moduli are of the same order of those expected from the estimations above. Moreover, the fits confirm that an increased exposure time to toluene softens the polymer and reduces its Young's modulus.

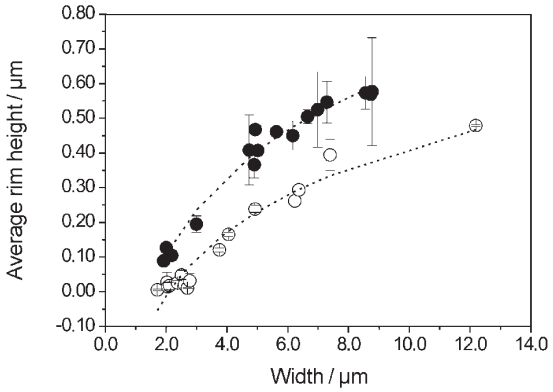

Figure 8. Average rim height versus width of microvessels on PS surfaces after overall softening times of ≈2 min (○) and 7–8 min (●) in toluene vapor and condensation of the water droplets. The dashed lines are fits based on the elastic theory for surface deformation (White[28]), as described in the text.

These conclusions are in agreement with the results obtained from the depth studies. Equation (2) states that the depth of the microvessel is independent from the width for constant contact angles. This can tentatively be understood as follows: the Laplace pressure, ΔP, is inversely proportional to the radius of curvature R of the droplet, that is, $\Delta P \sim 1/R$. Young's modulus is the ratio of the tensile stress exerted on a solid and the tensile strain, that is, the ratio of the force, F/A_0, exerted on a unit area A_0 of the substrate, divided by the strain, $\Delta L/L_0$, the relative elongation. This provides for the force: $F = (EA_0/L_0\Delta L) \sim \Delta L$. Here, ΔL can be identified with the depth, d, and F originates from the Laplace pressure. Therefore, $\Delta P \sim d$ and $d \sim 1/R$; the depth of the microvessels should increase for smaller water droplets. However, if the droplet is smaller it replaces less material in the substrate for the same contact angle. This scales with $d \sim R$. Both effects together provide a constant depth. A stronger contribution from the Laplace pressure comes into play only for radii of curvature in the order of h_0, which is usually on length scales far below 1 μm. The experimental results for the depth as function of the width of the microvessels are shown in Figure 9a.

For long exposure times to toluene (i.e. about 7–8 min), the depth increases with the width of the microvessels, whereas for short exposure times (≈2 min), it increases and reaches a plateau value for widths above about 3 μm. In Figure 9b, the

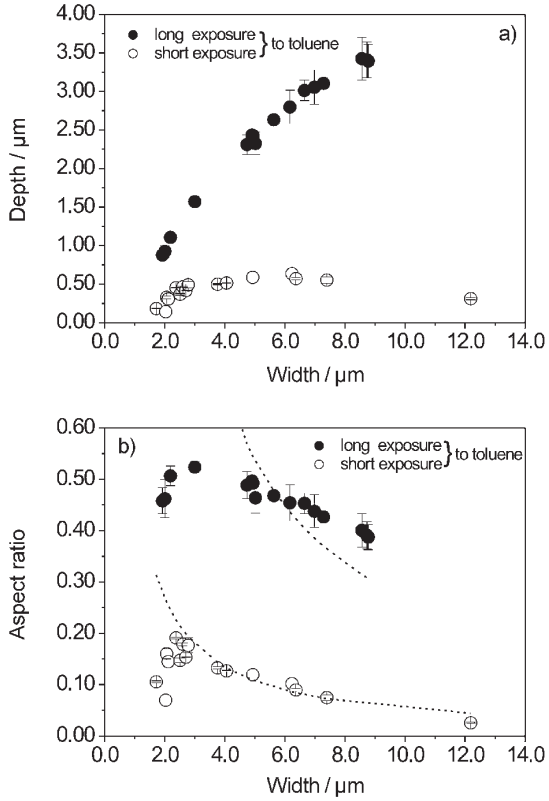

Figure 9. a) Depth of microvessels formed at a polystyrene surface after short (≈2 min) and long (≈7–8 min) exposure times to toluene vapor and condensation of the water droplets. b) Aspect ratio (depth/width) as a function of the width of the corresponding microvessels. The depth is taken below the surface (see Figure 2b) and thus does not include the rim height. The dashed lines are fits based on Equation (2).

aspect ratio is plotted versus the width of the microvessels for two different exposure times to toluene. In both cases, the aspect ratio of the microvessels decreases with the width. As for the depth, the aspect ratio for the shorter exposure time is lower than that for the longer one.

At longer exposure times, the polymer is softer and must have a lower Young modulus. According to Equation (2), this must lead to deeper vessels. However, according to this same equation, the depth should be independent of the width for a constant contact angle. This requirement is fulfilled in the case of shorter exposure times to toluene (neglecting the data below 3 µm). In contrast, the depth obtained at longer exposure times shows a strong dependence on the width. This mismatch between long and short exposure times is even more pronounced for the aspect ratio. According to Equation (2), the aspect ratio should be proportional to w^{-1}, as can be seen if both sides of the equation are divided by the width. A fit to the curves in Figure 9b, neglecting data below 3 µm, provides the same fit parameter A from the fits of the rim height (for $\theta = 90°$). As a result, Young's modulus is 242 and 47 kPa for the short and long exposure times, respectively. While the decrease can be attributed to the softening of PS, only the fit for the short exposure time is reasonable. In contrast, for the longer exposure time the dependence of the aspect ratio on the width is too weak.

This finding can be understood if we consider that small droplets evaporate faster than bigger ones. Therefore, after longer exposure times to toluene, the evaporation time of a small droplet is short compared to the long drying time of the PS substrate. Thus, the action of the droplet will be lost before the concave structure can be frozen; the PS surface equilibrates and the depth is lower than expected from the elastic theory. This interpretation is supported by the decrease of the aspect ratio for very small droplet sizes for both exposure times. The droplets evaporate so fast that the PS surface always flattens during drying. This explanation is supported by drying experiments of small PS particles.[19] There, drying from 180 to about 120% of the initial mass of the particle took approximately 2 s, which is approximately the evaporation time required for micrometer-sized droplets. Much smaller droplets evaporate faster, and flattening of the concave structure is favored. Much bigger droplets evaporate slower and the elastic deformation of the PS surface is frozen. Therefore, competition between the two processes—and thus, a strong influence of drying on the final surface structure—is likely to occur for small droplets.

A viscous drag of polymer chains to the rim of the microvessels may occur in addition to the elastic contribution to structuring. For this, polymer chains have to diffuse to the point of action. With a diffusion coefficient of $2\times10^{-13}\,m^2\,s^{-1}$ for PS ($M_w = 340$ kDa) in a toluene-rich PS matrix ($M_w = 220$ kDa), assuming a density of $\approx 1\,g\,mL^{-1}$ and a concentration of 50 weight%, the polymer chains might migrate $(6Dt)^{0.5} = 15$ µm in 3 min.[24] Since this is one order of magnitude larger than the dimensions of the microvessels, a viscous contribution to the structuring cannot be excluded.

Our experimental conditions for the last experiment resemble those for the generation of breath figures.[39,40] However, two characteristics in the breath figures disagree with our observations: 1) the missing rims as we observed it and 2) the well-ordered arrangement of the concave structures. The order was discussed to be caused by sinking and ordered packing of the droplets within the liquidlike polymer substrate. Indirectly, this discrepancy confirms that our substrate is still solidlike in most cases, and elastic theory is applicable—apart from the situation for longer exposure times and smaller droplets (see Figure 9b, filled circles). There, the aspect ratio is about 0.5, which is expected for a half-sunk spherical droplet. This result could be indicative of the initial step of a breath-figure-like effect.[41]

3. Conclusions

We investigated the formation of microcraters on soft PS surfaces by the action of sessile droplets of nonsolvents. The PS substrates were softened using toluene vapor. To understand which physical processes were responsible for the structuring, we controlled the exposure to toluene vapor and the deposition of the droplets. In the first experiment, droplets of slow evaporating EG/H_2O (with diameters of the order of 100–200 µm) were deposited by using the ink-jet technique,

followed by exposure to toluene. In this way, microcraters were formed as a result of the permanent uptake of toluene by the PS substrate outside the parts masked with the droplets. This led to a local expansion of the polymer. Aspect ratios of only 0.007 were obtained after drying. These aspect ratios could only be increased by means of a longer exposure time of PS to the toluene vapor or by decreasing the width of the microcraters.

In the second experiment, we condensed droplets of pure water (with diameters of the order of several micrometers) on the toluene-softened PS surface. Microcraters were formed as a result of the combination of the Laplace pressure exerted by the droplets on the soft PS surface and the surface tension of the droplets, which pulls the soft polymer upwards at the three-phase contact line to form a rim. In this way, the obtained aspect ratios were as high as about 0.5. This value occured owing to the superposition of three effects, namely, the permanent uptake of solvent, the scaling-down of the width of the microcraters, and the Laplace pressure. These results show that the combination of different physical phenomena can increase the aspect ratio, even for the system PS/toluene, without the need for polymer compaction or an additional coffee-stain-like flow of polymer to the rim.

We applied an elastic theory to fit the rim height and the depth versus the width of the microcraters. The fits provided reasonable values of the Young modulus for the soft PS surface. Even if the viscous contributions are neglected, these results show that surface structuring of polymers by solvents can be understood quantitatively. This quantification is an important step for a directed use of ink-jet etching as a tool for micro- or nanostructuring of polymers.

Acknowledgements

We gratefully acknowledge fruitful discussions with Prof. Werner Steffen, Prof. George Floudas, Dr. Kaloian Koynov, and Thomas Haschke. EB and RPC acknowledge the Max Planck Society (MPG) for financial support. R.P.C. further thanks the Swiss National Science Foundation for funding (Project No. PBGE2-112884).

Keywords: interfaces · nanostructures · polymers · scanning probe microscopy · surface analysis

[1] C. H. Liu, J. A. Zapien, Y. Yao, X. M. Meng, C. S. Lee, S. S. Fan, Y. Lifshitz, S. T. Lee, *Adv. Mater.* **2003**, *15*, 838–841.
[2] S. Karabasheva, S. Baluschev, K. Graf, *Appl. Phys. Lett.* **2006**, *89*, 031110.
[3] R. Pericet-Camara, A. Best, S. K. Nett, J. S. Gutmann, E. Bonaccurso, *Opt. Express* **2007**, *15*, 9877–9882.
[4] J. Aizenberg, A. J. Black, G. M. Whitesides, *Nature* **1999**, *398*, 495–498.
[5] H. A. Biebuyck, G. M. Whitesides, *Langmuir* **1994**, *10*, 2790–2793.
[6] T. Kawase, H. Sirringhaus, R. H. Friend, T. Shimoda, *Adv. Mater.* **2001**, *13*, 1601–1605.
[7] S. M. Senkan, *Nature* **1998**, *394*, 350–353.
[8] E. Bonaccurso, H.-J. Butt, B. Hankeln, B. Niesenhaus, K. Graf, *Appl. Phys. Lett.* **2005**, *86*, 124101.
[9] B. J. de Gans, S. Hoeppener, U. S. Schubert, *Adv. Mater.* **2006**, *18*, 910–914.
[10] R. D. Deegan, O. Bakajin, T. F. Dupont, G. Huber, S. R. Nagel, T. A. Witten, *Nature* **1997**, *389*, 827–829.
[11] C. Stupperich-Sequeira, K. Graf, W. Wiechert, *Math. Comput. Model. Dyn. Syst.* **2006**, *12*, 263–276.
[12] G. Li, H.-J. Butt, K. Graf, *Langmuir* **2006**, *22*, 11395–11399.
[13] G. Li, N. Hoehn, K. Graf, *Appl. Phys. Lett.* **2006**, *89*, 241920.
[14] E. Bormashenko, R. Pogreb, A. Musin, O. Stanevsky, Y. Bormashenko, G. Whyman, O. Gendelman, Z. Barkay, *J. Colloid Interface Sci.* **2006**, *297*, 534–540.
[15] T. Haschke, W. Wiechert, K. Graf, E. Bonaccurso, G. Li, F. T. Suttmeier, *Nanoscale Microscale Thermophys. Eng.* **2007**, *11*, 31–41.
[16] C. M. Bates, F. Stevens, S. C. Langford, J. T. Dickinson, *J. Mater. Res.* **2007**, *22*, 3360–3370.
[17] C. S. Yang, P. S. Ma, F. M. Jing, D. Q. Tang, *J. Chem. Eng. Data* **2003**, *48*, 836–840.
[18] E. Bonaccurso, H.-J. Butt, K. Graf, *Eur. Polym. J.* **2004**, *40*, 975–980.
[19] R. Zhang, K. Graf, R. Berger, *Appl. Phys. Lett.* **2006**, *89*, 223114.
[20] S. Alsoy, J. L. Duda, *Drying Technol.* **1998**, *16*, 15–44.
[21] J. C. Moreira, N. R. Demarquette, *J. Appl. Polym. Sci.* **2001**, *82*, 1907–1920.
[22] C. M. Stafford, C. Harrison, K. L. Beers, A. Karim, E. J. Amis, M. R. Vanlandingham, H.-C. Kim, W. Volksen, R. D. Miller, E. E. Simonyi, *Nat. Mater.* **2004**, *3*, 545–550.
[23] G. Floudas, W. Steffen, E. W. Fischer, W. Brown, *J. Chem. Phys.* **1993**, *99*, 695–703.
[24] T. Cherdhirankorn, S. Karabacheva, K. Koynov, G. Fytas, *Proceedings of the 2nd International Conference on Advances in Petrochemicals and Polymers*, Bangkok (Thailand), **2007**.
[25] S. Pickup, F. D. Blum, *Macromolecules* **1989**, *22*, 3961–3968.
[26] T. Krüger, F.-T. Suttmeier, W. Wiechert, R. Zhang, R. Berger, K. Graf, unpublished results.
[27] M. Rusdi, Y. Moroi, H. Nakahara, O. Shibata, *Langmuir* **2005**, *21*, 7308–7310.
[28] L. R. White, *J. Colloid Interface Sci.* **2003**, *258*, 82–96.
[29] R. von Klitzing, *Adv. Colloid Interface Sci.* **2005**, *114*, 253–266.
[30] J. T. Seitz, *J. Appl. Polym. Sci.* **1993**, *49*, 1331–1351.
[31] H. G. H. van Melick, L. E. Govaert, H. E. H. Meijer, *Polymer* **2003**, *44*, 2493–2502.
[32] S. K. Kaliappan, B. Cappella, *Polymer* **2005**, *46*, 11416–11423.
[33] G. V. Lubarsky, M. R. Davidson, R. H. Bradley, *Surf. Sci.* **2004**, *558*, 135–144.
[34] M. E. R. Shanahan, P. G. de Gennes, *C. R. Acad. Sci. Ser. II* **1986**, *302*, 517–521.
[35] E. R. Dufresne, D. J. Stark, N. A. Greenblatt, J. X. Cheng, J. W. Hutchinson, L. Mahadevan, D. A. Weitz, *Langmuir* **2006**, *22*, 7144–7147.
[36] D. Hull, B. D. Caddock, *J. Mater. Sci.* **1999**, *34*, 5707–5720.
[37] A. I. Rusanov, *Colloid J. USSR* **1975**, *37*, 614–622.
[38] *CRC Handbook of chemistry and physics*, CRC, Boca Raton, **1983–1984**.
[39] U. H. F. Bunz, *Adv. Mater.* **2006**, *18*, 973–989.
[40] B. H. Zhao, J. Zhang, H. Y. Wu, X. D. Wang, C. X. Li, *Thin Solid Films* **2007**, *515*, 3629–3634.
[41] L. Song, R. K. Bly, J. N. Wilson, S. Bakbak, J. O. Park, M. Srinivasarao, U. H. F. Bunz, *Adv. Mater.* **2004**, *16*, 115–118.

Received: February 18, 2008
Revised: May 16, 2008
Published online on July 23, 2008

